Journal of Atmospheric and Solar–Terrestrial Physics 214 (2021) 105532

Contents lists available at ScienceDirect

Journal of Atmospheric and Solar-Terrestrial Physics

journal homepage: www.elsevier.com/locate/jastp

Toward a theory of ball lightning occurring in houses and aircraft

John J. Lowke [a,*], Wilfried Heil [b], Eugene Tam [a], Anthony B. Murphy [a]

[a] CSIRO Manufacturing, Box 218, Lindfield, NSW, 2070, Australia
[b] Berlin, Germany

ARTICLE INFO

Keywords:
Ball lightning
Gas discharge
Metastable oxygen molecules
Singlet delta oxygen

ABSTRACT

Gas discharge properties have been calculated, considering electrons, negative ions, positive ions and the metastable singlet delta oxygen molecules, to assess the possibility of ball lightning resulting from an electrical discharge. It is found that if the metastable molecules have very large densities of the order of 10^{17} cm^{-3}, a stable ball-like plasma of electrons, positive ions, negative ions and metastable molecules is obtained, with electron densities of $\sim 10^{11}$ cm^{-3}. The ball can exist independent of the electrodes. There is an equilibrium within the ball between the detachment of electrons from negative ions by the metastables and the re-attachment of electrons to oxygen atoms reforming negative ions. As the ball is highly conducting, electric fields within the ball are very low. Such a high density of metastable molecules could be accumulated from corona pulses from a high voltage point within any structure such as a house or aircraft fuselage. Large electric fields would be present at the tips of such metal conductors within an ambient electric field existing during a thunderstorm. It is also calculated that significant electric fields exist at the edges of the plasma ball to match the ball potential with the ambient potential and that these fields can be sufficient to excite further metastable molecules and increase the ball lifetime.

1. Introduction

Ball lightning (BL) within houses and aircraft has been observed by hundreds of people, who report approximately similar properties. The ball is a few centimetres in diameter, moves at about walking speed, emits light that is easily observable in daylight but is not so bright as to hurt the eyes, lasts about 10–40 s, and frequently first appears from closed glass windows. Of a survey by Piccoli and Blundell (2014) of 286 observations in France, 185 were from the inside of houses or aircraft. Of these reported observations, remarkably few reported any damage or injury. One observation, from the pilot of a DC3 aircraft and reported to JJL and ABM, was of BL passing down the central aisle of the aircraft while an air hostess standing in the aisle reported no sensation, even heat, as the ball passed around her legs and continued along the central aisle. However, there is one reliable account differing from these injury-free reports; Selvaggi et al. (2003). "During a great storm" a 28-year-old father in the living room of his Belgian farmhouse, while "adjusting wood and papers in an open fireplace", experienced BL coming out of the fireplace, which hit him causing him to lose consciousness and second-degree burns on his hand. The ball, as reported by his wife, then continued and caused third-degree burns affecting 30% of the body of his 5-year-old daughter, requiring treatment in hospital for 37 days. We discuss this incident further in Section 6.

It has been most challenging to explain the observed properties in terms of conventional gas discharge theory, or indeed any theory. How can such discharges be initiated inside a house, and even an aircraft with a metal fuselage that is similar to a "Faraday Cage"? What is the energy source for the light output lasting 10 s or more? Why does BL almost invariably move, over distances of many metres, sometimes along a complex path through open doors and passages? There are even reputable reports of BL passing through closed glass windows. Many previous efforts to explain these phenomena have resorted to explanations involving rare physical processes, for example involving antimatter, black holes, relativistic electrons, magnetic knots, microwave radiation, atmospheric masers, nuclear particles and oxidizing polymers; for references proposing each of these processes see Lowke et al. (2012); Bychkov (2002); Shmatov and Stephan (2019).

The most quoted theories involve the oxidation or burning of a minority component, such as silicon or carbon, e.g. Abrahamson and Dinnis (2000). It is difficult to invoke an oxidation mechanism to explain BL occurring inside structures, because of the lack of evidence of either the origin or the remnants of any oxidation material. In the present paper, we propose that the active component is the "singlet delta" or first excited state of the oxygen molecule, which is metastable. There are

* Corresponding author.
E-mail addresses: john.lowke@csiro.au, john.lowke@unisa.edu.au (J.J. Lowke), tony.murphy@csiro.au (A.B. Murphy).

https://doi.org/10.1016/j.jastp.2020.105532
Received 27 November 2020; Received in revised form 22 December 2020; Accepted 25 December 2020
Available online 15 January 2021

then no visible sources or products, consistent with most observations of BL inside structures. The important role of excited states has been mentioned previously. For example, O'Doherty (1944), in discussing circuit interruption, said "excited atoms or molecules can exist for appreciable times after current has been interrupted", and Powell and Finkelstein (1969) proposed metastables to explain their results for radio-frequency discharges, as is discussed later.

Throughout this paper, when the term "metastables" is used, we are referring to just the one electronically excited state of oxygen molecules, called the singlet delta state, designated as $O_2(^1\Delta_g)$, with an excitation energy of 0.98 eV. Its cross-section for excitation in air is known as a function of electron energy (Lowke, 1992) and significant excitation occurs for electric fields as low as 2 kV cm^{-1}. Fig. 1 show metastable excitation coefficients relative to ionization and attachment coefficients for air at 1 bar. A crucial property of these metastables is that they detach electrons from negative oxygen ions, the detachment rate being 2.0×10^{-10} cm^3 s^{-1}; (Lowke, 1992). The metastable state has a radiative lifetime of about 45 min, and known quenching rates with oxygen, water vapour and nitrogen of 2.22, 5.6 and < 0.003 cm^3 s^{-1} respectively; (Findlay and Snelling, 1971). Excitation of these metastables, and thus electron detachment from negative ions, explains the reduction of the sustaining electric field of discharges in air from 25 kV cm^{-1} at breakdown to ~5 kV cm^{-1} after initial breakdown; (Lowke, 1992). Recent interest in this molecular state has grown because of its possible central role in the beneficial treatment of cancer tumours by plasmas (Bauer and Graves, 2016).

The proposal that oxygen metastables are the essential active component of BL explains the three previously unexplained questions about BL in structures. Namely, how does it get inside a house, what is the energy source of the ball, and what determines its lifetime? The metastables can be formed if a high voltage point exists on metal inside of the house or aircraft. The discharge can be very small, i.e. only 1 mm in diameter, and almost noiseless and invisible. The energy of the metastables provides the energy that allows the ball to give out light. The number of metastables determines the lifetime of the ball. Metastables detach electrons from negative oxygen ions, which enables the formation of a moderately high density of electrons. An equilibrium can be reached between electrons forming from detachment from oxygen and being lost by re-attachment to oxygen molecules. There is no need for any background electric field. The ball is then independent of electrodes, and the metastable density decreases slowly.

To examine the plausibility of this proposal, we consider electrons, positive and negative ions and singlet delta oxygen metastables, with the metastables produced only by direct electron excitation. In a discharge plasma, the physical processes are much more complex, as has been described in detail in the review article of Ionin et al. (2007), which considers many excited states of oxygen and 97 separate reactions between these particles. Inclusion of these additional processes, mentioned on pages R30, R45 and R29 of the review, would improve the viability of the metastable hypothesis in three respects.

a) Higher excited levels such as the O(^{1}D) state and the $O_2(b^1\sum_g^+)$ state also contribute to the formation of singlet delta molecules by collisions with ground-state oxygen molecules.
b) Strong experimental evidence exists that energy transferred from the nitrogen vibrational states, which are also metastable, increases the production of singlet delta metastable oxygen molecules by up to a factor of 10!
c) Direct radiation from the relaxation of metastable state of oxygen, being of energy 1 eV, would give infrared photons of wavelength 1.27 μm and thus not contribute to visible radiation. However, it is firmly established that binary collisions of metastable molecules produce photons of double the energy, with a wavelength of 762 nm, in the red region of the spectrum. There is also evidence at high densities of triple-body collisions delivering photons of energy ~3 eV at ~500 nm in the yellow region of the spectrum.

An earlier review of the physical properties of singlet delta oxygen molecules has been given by Kearns (1971).

Tesla (1944), in his laboratory notes, reported the production of "fireballs" of up to 1.5 inches (38 mm) in diameter from the terminals of his experimental equipment. This equipment produced radio frequency voltages of up to 2 MV, at a frequency of 150 kHz and consisted of a high-voltage transformer, several resonant circuits and a rotating spark gap. These experiments have been repeated by two brothers, K L and J K Corum, who published these results as a demonstration of the experimental production of BL (Corum and Corum, 1990). The balls lasted a few seconds, with a number of balls appearing successively in the same experiment. Several balls were described as giving the "appearance of passing through glass". Metastable oxygen molecules would have been excited in these experiments.

Metastable excitation was previously proposed by Powell and Finkelstein as a possible explanation of the behaviour of the experimental discharges they obtained in air by radio-frequency excitation, which they proposed as being similar to BL (Powell and Finkelstein, 1969). After termination of voltages from the power supply, these discharges lasted about half a second and rose upwards, presumably from convection resulting from the plasma being above room temperature. In our model, the metastables are initiated by corona pulses, for which the discharge is only active for about 10% of the time, as illustrated later in Fig. 9 and for which heating is much less.

The present paper is in some respects similar to the recent papers of Morrow (e.g. Morrow, 2018, 2019), which also investigate the possibility of BL being a gas discharge by solving conventional gas discharge equations. In both Morrow's model and ours, the main ball consists of positive and negative ions. In Morrow's model, applicable for BL outside of structures, burning particles need to be added to provide light output. In our model, excited metastables are the active component. The present paper is an extension of the earlier paper of Lowke et al. (2012), that considered the effect of metastable oxygen molecules. Instead of representing the effect of the increase in the electron density from metastable detachment by an arbitrary increase in the ionization coefficient, the present paper calculates the detailed production and destruction of metastable densities as a function of time and position throughout the discharge.

A recent paper of Shmatov (2020) gives a reference to a video recording the formation and disappearance of volumes of light-emitting air within thunderclouds. Such phenomena may also be consistent with

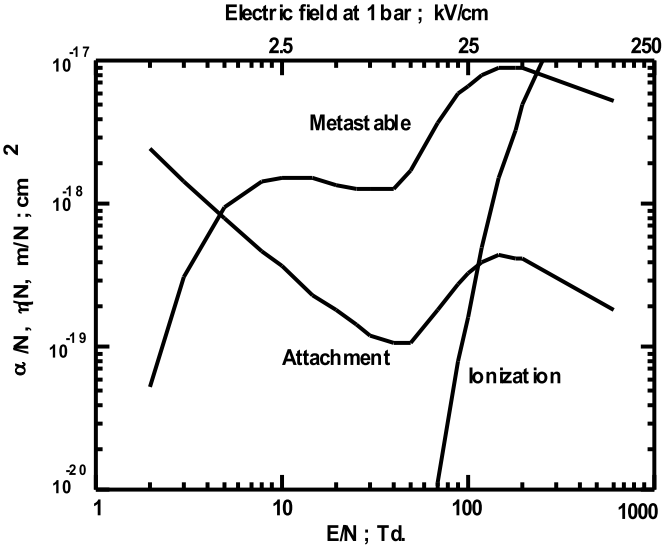

Fig. 1. Coefficients of electron excitation of metastables, electron attachment to air molecules, and ionization in air, at 1 bar (from Lowke, 1992).

the present model if many cylindrical particles of ice less than a millimetre in diameter accentuate electric fields at their tips to create discharges, as proposed by Dubinova et al. (2015), and produce large numbers of metastables. The metastables, if at high density, could detach electrons from negative ions and produce large volumes emitting light.

Section 2 presents calculations of the intensification of an ambient electric field that can occur at the tips of conducting cylinders. Such conductors can exist within a structure, for example, conducting pipes within a house or the fuselage itself for an aircraft. Section 3 gives detailed calculations of pulsed corona development, including details of metastable production, from such conductors. Such pulse development was described earlier by Trichel (1938), and the pulses are frequently referred to as "Trichel pulses". We consider a potential of 14 kV on a metal region around 2 mm in diameter, for example, at a metal window frame. Metastables accumulate in the discharge from each current pulse.

Section 4 describes properties of discharges if the metastable particle densities accumulate to very large values of $\sim 10^{17}$ cm^{-3}. Such high densities of metastable oxygen molecules have been measured previously in plasmas for biological applications, (e.g. Sousa et al., 2013). The detachment of electrons from negative ions by such a cloud of metastables produces a cloud of electrons. This central ball, being a conductor, has an almost zero electric field within it and can, we propose, exist for some seconds independent of the electrodes and have properties similar to BL. Quenching rates of metastables predict that the half-life of such a ball would be less than a second. However, Section 5 gives calculations showing that a source of additional metastable excitation and also ionization arises from electric fields that are increased a factor of two in the sheath regions at the edge of the ball, arising from the ambient electric field interacting with the ball.

Sections 6 and 7 discuss and summarize the calculations, which are incomplete in that they do not span in detail the transitions between the different stages of discharge development. We also give no analysis of the production of visible radiation. Hence, we have called our paper "Toward a theory of ball lightning". A brief account of the theory has been given previously (Lowke, 2019). The appendices give detailed observations of BL initiated by metal columns, for an aircraft fuselage in Appendix 1 and a metal pipe in a house in Appendix 2.

In Appendix 1, Don Smith gives more detail than previously (Lowke et al., 1996) of the observation of BL in a US transport aircraft in which he was the navigator. A description is given of (1) corona produced at the aircraft's radome immediately prior to the observation of BL, (2) the exact position of the initial formation of BL within the cockpit, which was near the metal post dividing the glass at the centre of the windshield, rather than at the glass itself and (3) details of the long travel path of ~55 m of the BL within the aircraft. Appendix 2 gives an account of BL initiated inside a house at the end of a steel pipe terminating in a sink at the end of the building, which could be explained by the field intensification at the end of a conductor, as described in Section 2.

2. Electric field amplification by conductors in structures

Ambient electric fields, such as from a thundercloud, cause charge movement within metal conductors, for example, the metal fuselage of an aircraft or metal plumbing within a house. These charge movements cause an enhancement of the ambient electric field just outside of the extremities of the conductors. Charges move inside the conductor until the electric field is zero within the conductor.

A useful assessment can be made of the magnitude of these effects by using the approximate relation that the enhancement factor of the ambient electric field at the tip of a cylinder of length L, capped by hemispheres of radius R is $L/2R$. This approximate relation can be derived by considering a metal cylinder of length $L/2$ and radius R above a ground plane within a uniform ambient electric field E_0. Charges Q are needed on the tip of the cylinder to balance the potential $E_0L/2$ from the ambient field. The potential from the charges is given by electrostatic theory as $Q/4\pi\varepsilon_0R$, where ε_0 is the permittivity of free space; equating this with $E_0L/2$ gives $Q = 4\pi\varepsilon_0RE_0L/2$. The electric field E from these charges follows from the derivative of the potential with respect to radius, and is $Q/4\pi\varepsilon_0R^2$, which on substitution for Q becomes $E = E_0L/2R$. For a "floating" cylinder totally immersed in a background field, the enhancement would be approximately the length of the cylinder divided by its diameter.

We have checked the accuracy of this approximate analytic expression by doing numerical calculations of field enhancement for a wide range of the ratios of length to diameter of conducting cylinders capped by hemispheres, for various uniform ambient electric fields and for both a floating and grounded cylinder within an electric field. Calculations are made for the electric potential φ by solving $\nabla\cdot(\sigma\nabla\phi) = 0$ using finite-difference methods, where σ is an effective electrical conductivity. As $\sigma\nabla\phi$ is current density, the equation imposes zero net current, as required under steady-state conditions. The electric field is obtained from the derivative of the potential. Outside of the cylinder, σ is set at 1, but inside of the cylinder we make $\sigma \sim 10^5$, to represent the very high electrical conductivity of the metal compared with the surrounding atmosphere. A non-uniform structured grid is used, with a finer grid in the immediate vicinity of the hemispherically capped cylinder. The dimensions of the grid increase in a geometric progression from the fine to the coarse mesh region, with a total of approximately 10^7 control elements. Results of these calculations are given in Fig. 2, showing that the simple formula is generally accurate to 20%.

The simple formula that the electric field is accentuated by $L/2R$ indicates that accentuations of more than a factor of 10 are possible and would occur with most aircraft as the ratios of fuselage length to diameter are more than a factor of 10. Fig. 3 shows calculated field accentuations for an Airbus, with a background field of 1 kV cm^{-1}, taken from Karch et al. (2017). At the extremities of the aircraft, calculated fields are ~25 kV cm^{-1}, an increase of a factor of 25. This is the field above which, from Fig. 1, ionization is greater than attachment, so that local corona is likely. Onset fields at lower pressures will be lower. The calculations are consistent with the frequent observations of corona at tips of the small diameter wires installed at the ends of some aircraft. The accentuation of electric fields is very large at the aircraft's radome, the non-metallic enclosure surrounding the radar equipment. There are usually metallic strips within the radome connected to the aircraft fuselage, to protect against the destruction of the radome by lightning. These metal strips, shown in Fig. 4, were the source of the "horns" of corona seen on the C-133 A aircraft reported in Appendix 1 and also reported in Lowke et al. (2012). The "horns" are indicated by the blue lines drawn on the photograph of Fig. 4. The presence of this corona

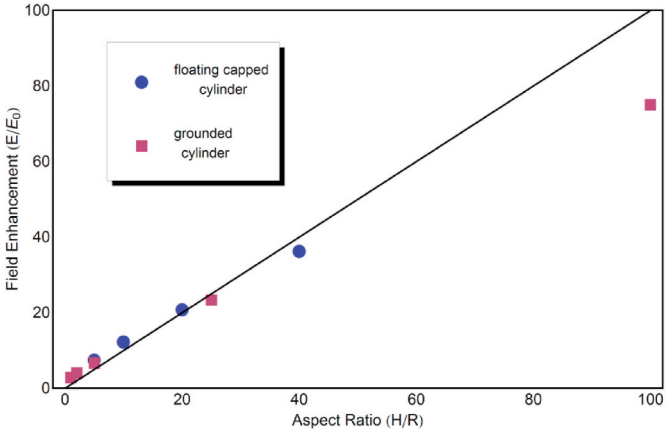

Fig. 2. Calculated field enhancement factor of background fields at the tips of conducting cylinders capped with a hemisphere; R is the cylinder radius and H is the cylinder length if one end is grounded and half of the cylinder length if "floating".

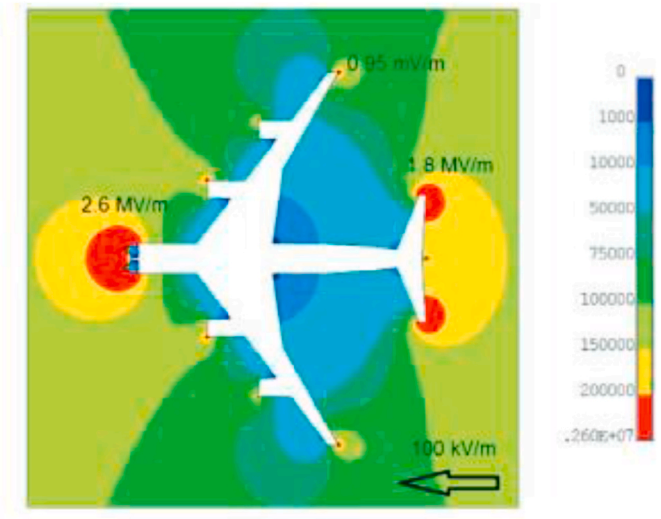

Fig. 3. Calculated electric fields surrounding an Airbus fuselage with an ambient electric field of 1 kV cm^{-1}. Fields are ~25 kV cm^{-1} at extremities of the fuselage; from Karch et al. (2017), with permission.

results from the existence of high fields at the extremities of the aircraft.

3. Predictions of corona pulses including metastable production

We assess the nature and magnitude of possible metastable production inside a structure by considering the discharge produced from a high potential on a small point within the structure. Discharges from a small point will be pulsed for voltages slightly above the onset voltage (Trichel, 1938). The calculated properties of such pulses are similar to those obtained previously, except that our calculations include predicted metastable densities. Pulsed discharges involve less heating than continuous discharges as the pulse has current only flowing for about 10% of the time. Thus, pulsed discharges are more likely to be able to simulate BL, which does not generally rise through natural convection, suggesting that BL is not significantly hotter than ambient temperatures. The radio-frequency plasmas of Powell and Finkelstein (1969) rose in the air, probably due to heating. Rather than implementing numerical procedures to represent a point, we simply choose voltage boundary conditions of 14 kV imposed over a central spot of radius 1 mm.

The present paper differs from the treatment of Lowke et al. (2012), in that the effect of increased electron densities, produced by metastables detaching electrons from negative ions, is not represented by the simple approximation of increasing the effective ionization coefficient. Instead, the metastable particle density is calculated as a function of time and position, accounting for electron excitation and metastable detachment, excitation and quenching. If metastable densities reach ~1% of the total densities at atmospheric pressure, i.e. ~10^{17} cm^{-3}, electron densities of the order of 10^{11} cm^{-3} are produced and have an appreciable effect on the electrical conductivity and structure of the discharge. Pulsed discharges can accumulate large densities of metastables through the action of successive pulses, as discussed in the next section.

The present paper also differs from Lowke et al. (2012), in that the driving electric field is not assumed to originate from the accumulation of charges on the outside surface of a glass window. Reasons are:

a) Don Smith's observation, described in Appendix 1, that the ball is formed over the central metal divider between separate glass panes of the pilot's window, rather than over the glass surface of the windowpane;

Fig. 5. Electric discharge on the surface of an aircraft window. Discharge path splitting indicates the discharge was initiated on the window frame rather than the glass. From YouTube/PilotsTubeHD, with permission.

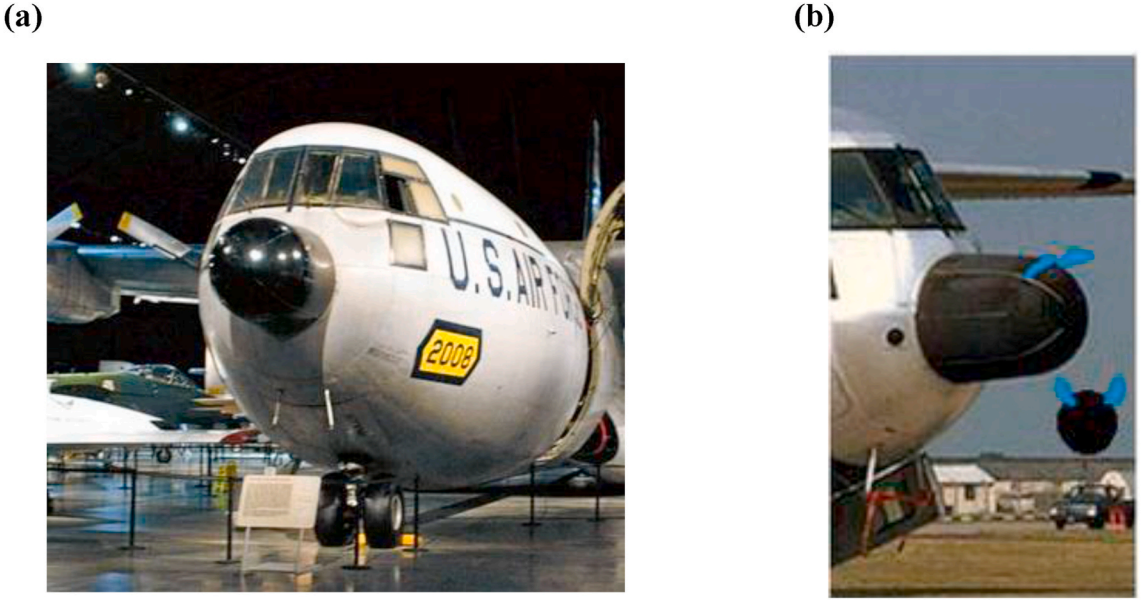

Fig. 4. (a) C-133 A cargo aircraft showing metal dividers in pilot's wind shield. (b) Shows corona "horns", marked in blue by Don Smith on black radome; Photos from US Air Force, Wright Patterson.

b) In a frame from a video of an electric discharge occurring at a pilot's window during a thunderstorm, shown in Fig. 5, branching of the electrical discharge indicates that the discharge originated from the window frame rather than the glass;
c) Modelling of discharges originating at a glass surface suggests that such discharges are terminated after a few pulses because the accumulation of charges on the glass surface reduces the electric field to below that necessary for ionization.

We calculate details of discharge development, from a point within the structure, such as on the metal divider within the windshield, that is influenced by the high electric fields immediately in front of the aircraft, as described in Section 2. It is assumed that such a point is not earthed, e.g. to the frame of the aircraft. The point is taken to be the initiating point of BL, as discussed in Appendix 1 for an aircraft and Appendix 2 for a house.

We solve for the development of the densities of the four major discharge constituents, namely electrons, n_e, positive ions, n_p, negative ions, n_i, and metastable particles, n_m, originating when the electric field near the point is such that ionization is greater than attachment, i.e. greater than 25 kV cm^{-1} at atmospheric pressure. The equations for the time dependence of the densities of these four particles are respectively (Lowke et al., 2012):

$$dn_e / dt = n_e\alpha W - n_e\eta W - \nabla\cdot(n_e W) - \gamma n_e\cdot n_p + k_d\cdot n_m\cdot n_i. \quad (1)$$

The terms on the right are for ionization, attachment, convective flow, recombination and detachment; α is the ionization coefficient, cm^{-1}, η the attachment coefficient, cm^{-1}, W the electron drift velocity, cm s^{-1}, γ the recombination coefficient, cm^3 s^{-1} and k_d the detachment coefficient, cm^3 s^{-1}.

$$dn_p / dt = n_e\alpha W - \nabla\cdot(n_p W_p) - \gamma n_e\cdot n_p - \gamma_i\cdot n_i\cdot n_p; \quad (2)$$

where W_p is the positive ion drift velocity, and γ_i the recombination coefficient for ions.

$$dn_i / dt = n_e\eta W - \nabla\cdot(n_i W_i) - k_d\cdot n_m\cdot n_i - \gamma_i\cdot n_i\cdot n_p; \quad (3)$$

where W_i is the negative ion drift velocity, and k_d is the detachment coefficient, cm^3 s^{-1}.

$$dn_m / dt = n_e \;\; mW - kq\; n_m\, N/5 - k_D n_i n_m + D\nabla^2 \;\; n_m; \quad (4)$$

where m is the coefficient for metastable production, cm^{-1}, analogous to α for electron production and η for ion production for air at atmospheric pressure; k_q is the quenching rate, cm^3 s^{-1}, D is the diffusion coefficient for metastables, cm^2 s^{-1} and N, cm^{-3}, is the density of the total number of gas molecules. The factor of five arises because we apply the quenching coefficient for oxygen, whose density is N/5.

Finally, there is the Poisson equation for the electric field accounting for space-charge effects:

$$\nabla\cdot E = (e/\varepsilon_0)(n_p - n_e - n_i); \quad (5)$$

E is the electric field, and e is the electronic charge. Potentials governing the discharge are determined by the ambient electric fields, the significant influence of conductors such as the aircraft fuselage on this field, and also the influence of space charge within the discharge, which is a complex function of space and time. Metastable molecules significantly alter the field within the discharge through detaching electrons from negative ions. Electrons have mobilities about 100 times larger than negative ions, thus changing the conductivity of this region of the plasma and the local electric field. Values of ionization, attachment and metastable production coefficients, α, η and m_i, as a function of the electric field, are shown in Fig. 1. We used $k_q = 2.22\times10^{-18}$, $k_d = 2.0\times10^{-10}$ and $\gamma = 2.0\times10^{-7}$ cm^3 s^{-1} and $D = 0.4$ cm^2 s^{-1}, sources for which are given in Lowke (1992).

The equations were solved in two-dimensional axisymmetric geometry, using 100 grid points for the radial and 200 grid points for the axial position in a horizontal cylindrical region of radius 40 cm and length 1.4 m. A non-uniform grid was used, with a minimum mesh size of 0.05 cm. Explicit numerical methods were used to solve the equations for particle densities, with upwind differencing used for the convective terms. For the Poisson equation, we used matrix inversion with successive iterative solutions of tri-diagonal matrices for both rows and columns.

In the calculations, the high-voltage point is represented by imposing a high-voltage boundary condition on a small circular area of radius 1 mm in the centre of a plane conducting surface, corresponding to the vertical axis of Fig. 6a. Pulses are obtained, rather than a continuous discharge. The potential of 14 kV represents the effective potential of the ambient electric field modified by conductors. This negative potential, for example at a point on a window frame, is effectively the "cathode". The boundary potential is reduced linearly from the central high-voltage region to zero on a region of radius 1 cm centred on the vertical axis of Fig. 6a. It is set at zero over all other boundaries. If the diameter of the high-potential spot were to be smaller, electric fields would be larger for the same potential, but the volume of the high-field region creating metastable molecules would be smaller. If the volume of the high-field region is too large, the time interval between pulses becomes large because of the time taken for charges to clear and thus restore the electric field for the next current pulse. There is then an unduly long time required for a sufficient number of pulses to accumulate a high density of metastable molecules.

The potential of 14 kV is low, considering that potentials within thunderclouds are thought to vary by 1 MV or more. Fig. 6b shows the calculated electric fields corresponding to Fig. 6a, which indicate the initial conditions of the calculations. The zero potential boundary condition is at a radius of 40 cm and at an axial length of 1.4 m. It is seen from Fig. 6b that the region of electric field greater than 2 kV cm^{-1} that is required to excite metastable molecules does not extend beyond 1 cm from the plane surface. The calculations would be little different if the axial length of the region of integration were 10 cm, rather than 1.4 m.

It was assumed that an initial electron density of 10^{-3} cm^{-3} existed throughout the volume to provide initiating electrons for starting the discharge. Calculated maximum values of the field at the centre of the left-hand plane from Fig. 6b, are ~40 kV cm^{-1}, which is well above the field of 25 kV cm^{-1} necessary to initiate ionization through the ionization coefficient being greater than the attachment coefficient. It was assumed that all fluxes of charged particles impinging on the conducting surface of the left-hand plane of Fig. 6a are absorbed by the surface. Other surfaces along the walls of the horizontal cylindrical region of integration are assumed to be insulating and retain surface charges from any impinging flux of charges. For the short times of the present calculations and large distances of the other boundaries from the high potential spot, such effects were not appreciable.

The high field of 40 kV cm^{-1} in front of the central area of the negative cathode plane causes rapid ionization so that after 0.6 μs a cloud of electrons, negative ions and positive ions is produced, with particle densities of ~10^{11} cm^{-3}. These densities are shown in Fig. 7a -7c and are at the time of the maximum current of the first pulse. Metastable densities, shown in Fig. 7d, are more than an order of magnitude higher than densities of electrons and ions because of the higher excitation coefficients for metastables shown in Fig. 1. Although the number of positive and negative charges that are created at ionization are equal, some of the positive charges are attracted to the cathode plane and are absorbed, as is shown in Fig. 7e and f, leading to local net positive and negative charge densities. It is the net charge density that determines local electric fields. Thus, the total number of positive ions is reduced, and the resulting increase in the net negative charge reduces the field in front of the cathode from 40 kV cm^{-1} in Fig. 6b to ~30 kV cm^{-1} in Fig. 7h. The overall potential of the discharge shown in Fig. 7g appear little changed from the initial potential shown in Fig. 6a, but it is the spatial derivative of this potential that determines the electric field and

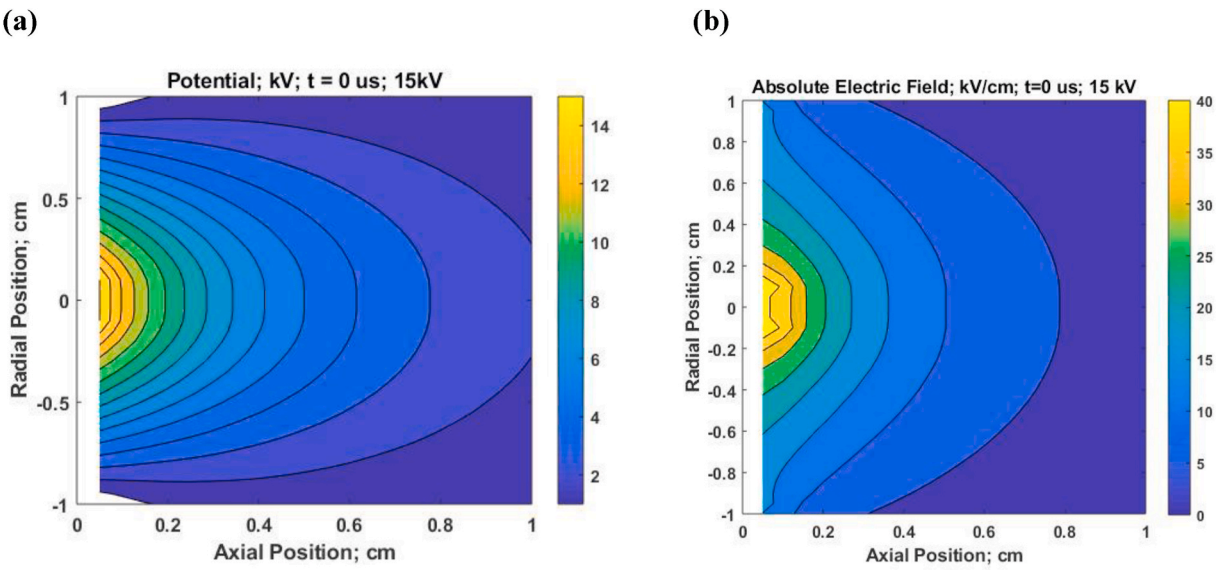

Fig. 6. Initial conditions of calculations of Fig. 7–10; (a) Input boundary potentials were 14 kV over 1 mm for zero radius and axial position and zero voltage at the outer radius of 40 cm and an axial position of 1.4 m; (b) Derived absolute value of initial electric field.

the character of the discharge.

Fig. 8 shows conditions at the later time of 2 μs, which is before the second current pulse. The electric field, given in Fig. 8h and is reduced still further to 20 kV cm^{-1}, below the field of 25 kV cm^{-1} necessary for ionization, because of the absorption of more positive ions at the cathode surface. Electron densities, shown in Fig. 8a, are reduced by attachment by a factor of 10^5 from Fig. 7a, to less than 10^7 cm^{-3}. As there is no net ionization producing electrons, the discharge is extinguished, apart from ion currents. Positive and negative charge densities of Fig. 8b and c are influenced by the absorption of positive charges at the cathode plane and also by repulsion of the negative charges away from the cathode plane. Metastable densities are further increased to $\sim 10^{13}$ cm^{-3} because metastable excitation from electrons occurs for fields as low as 2 kV cm^{-1}. When most of the positive ions are absorbed by the cathode surface, and negative ions have been repelled from this surface, the strong electric field of Fig. 6a is restored, and there is a second pulse.

We can compare initial conditions, shown in Fig. 6, with those at the current pulse maximum in Fig. 7 and conditions between the current pulses in Fig. 8. The structure of the voltage distributions in Figs. 6a, 7g and 8g is little changed. However, electron densities are substantial in Fig. 7a and effectively zero in Fig. 8a. The distributions of net charge densities in Fig. 7e and f differ substantially from those in Fig. 8e and f. The electric fields at the cathode surface change from being well above the ionization field of 25 kV cm^{-1} in Figs. 6b and 7h to falling below this field at the end of the ionization pulse as shown in Fig. 8h. The metastable densities of Figs. 7d and 8d show a continuous increase while there are electrons present, reaching $\sim 10^{13}$ cm^{-3} after just one pulse, compared with the negative ion densities of 10^{11} cm^{-3}. The metastable densities accumulate with each pulse.

Fig. 9 shows the calculated form of the current pulses as a function of time, obtained by simply plotting the maximum electron density in the whole discharge as a function of time. The frequency of the pulses is highly dependent on the high-voltage electrode configuration. It is seen that the conducting time for the pulses is only about 10% of the total time. The time between pulses for the calculations of Figs. 7 and 8 is ~6 μs, which enables many pulses to form in a few seconds during which time the accumulation of metastables will be substantial.

4. Accumulated metastables produce a stable "ball" of electrons and ions

We now consider the effects of an accumulation of metastables after many pulses. The principal effect of the metastable oxygen molecules is to detach electrons from negative ions. These detached electrons reattach to oxygen molecules in less than 0.1 μs to again form negative ions, so that at low metastable densities there are negligible changes to properties of the discharge.

However, there are very significant changes to the discharge if a high metastable density accumulates. After about a microsecond, an equilibrium develops between the rate of formation of detached electrons from metastables colliding with negative ions, $k_D\ n_m\ n_i$, and the rate of loss of electrons from their attachment to form negative ions, $n_e\ \eta\ W$. Both rates are given in equation (1). In the centre of the ball, the electric field is near zero and ionization, and convective flow can be neglected. An approximate relationship is obtained by equating these rates of attachment and detachment, which upon rearrangement gives

$$n_e/n_i = k_D\ \ n_m/\eta \mathrm{W} \tag{6}$$

The attachment rate constant ηW is finite at zero electric field when $W = 0$. Substituting for k_D and using $\eta = 40$ cm^{-1} and $W = 10^6$ cm s^{-1} for the low field value of $E/N = 2$ Td (1 Td = 10^{-17} V cm^2) from Figs. 4 and 5 of Lowke (1992), we obtain $n_e/n_i \sim 10^{-17}$ n_m. This relationship shows that, for small values of n_m, the electron density is negligible compared with the negative ion density.

However, for values of the metastable density n_m greater than 10^{17} cm^{-3}, equation (6) indicates that the electron density becomes greater than the negative ion density, which is typically 10^{11} cm^{-3}. This high density of electrons is quite stable as the rapid attachment of electrons to oxygen molecules to form negative ions is balanced by the high density of the metastables, which detach the negative ions and restore the high electron density. The shape of the cloud of electrons is the same as the accumulated cloud of metastable molecules, which will be approximately spherical due to diffusion. The diffusion coefficient of metastables in air is 0.2 cm s^{-1}, which from our calculations is high enough to make the cloud of metastables approximately spherical over ~10 s but not so high as to disperse the cloud.

At this high electron density, the electrons constitute a highly conducting ball and change the whole structure of the discharge. Because the electron ball is highly conducting compared with the rest of the

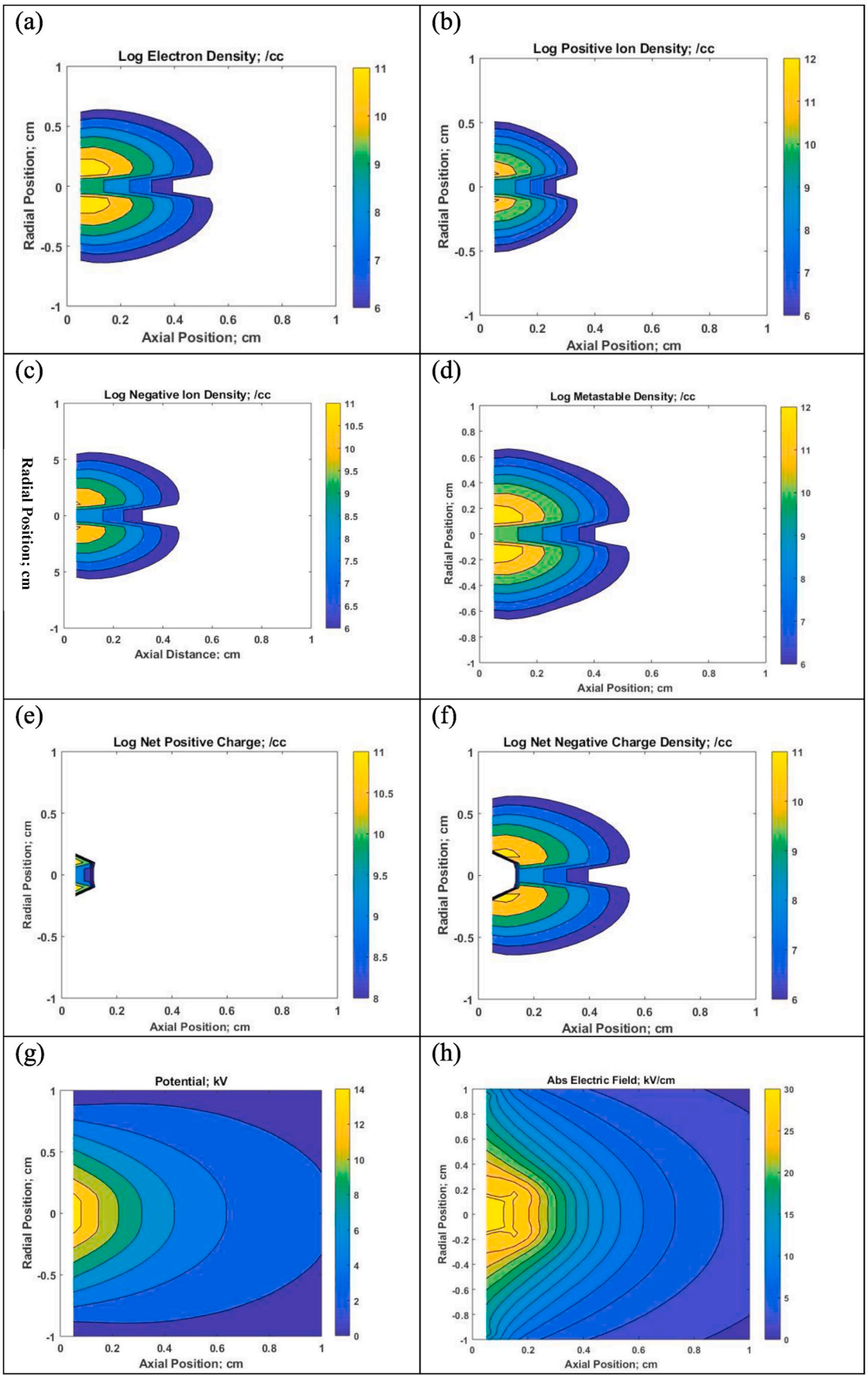

Fig. 7. Calculated distributions of (a) electron density, (b) positive ion density, (c) negative ion density, (d) metastable density, (e) net positive charge density, (f) net negative charge density, (g) electric potential, (h) absolute value of electric field; at maximum of first current pulse; 0.6 μs.

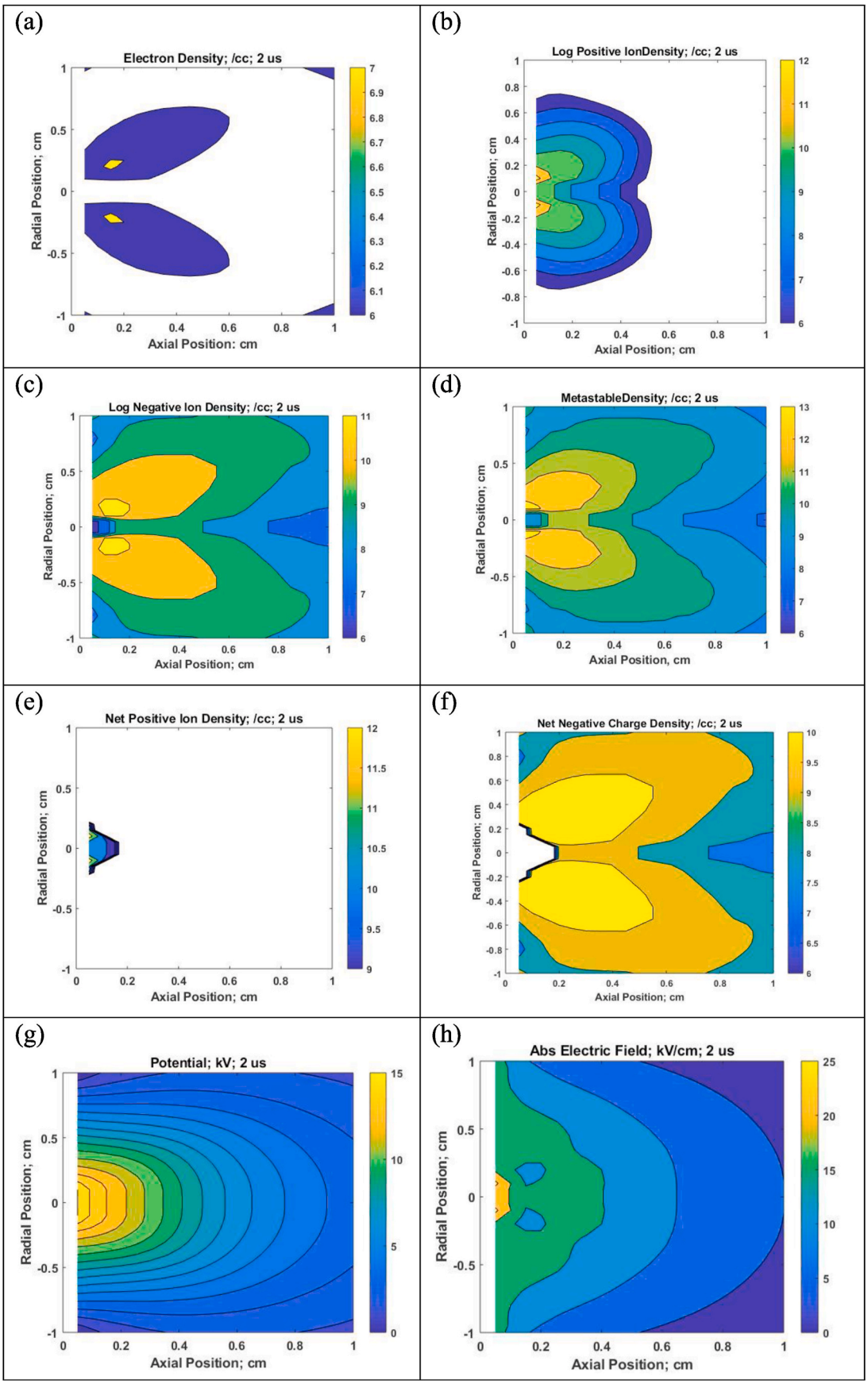

Fig. 8. Calculated distributions of (a) electron density, (b) positive ion density, (c) negative ion density, (e) net positive charge density, (f) net negative charge density, (g) electric potential, (h) absolute value of electric field; before second pulse; 2 μs.

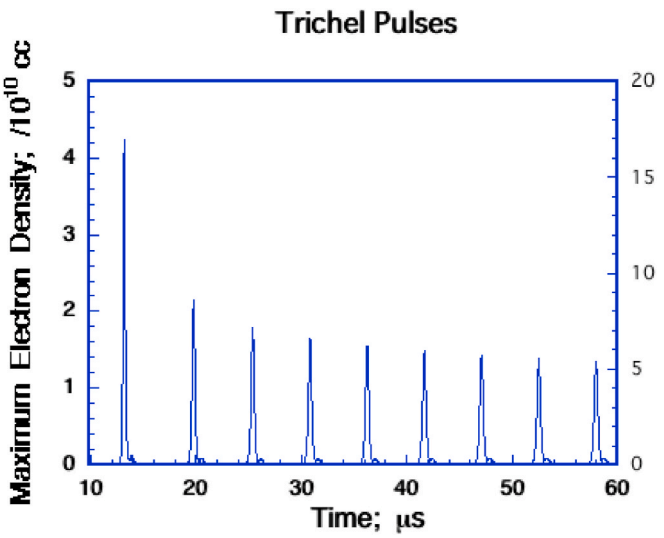

Fig. 9. Current pulses – corresponding to Fig. 7 and 8.

discharge, the electric field within the ball is very low. Numerical calculations of the magnitude of these effects are shown in Fig. 10. The results were obtained by numerically introducing a 1 cm diameter ball of metastable particles, of density 10^{17} cm^{-3}, into the discharge space of Fig. 8, as shown in Fig. 10d. We also set the positive and negative ion densities within the ball to 10^{11} cm^{-3}, these being typical ion densities in discharges, as shown in Fig. 8b and c. In less than 1 μs, electron detachment by the metastable molecules cause electron densities within the ball to increase from near zero to ~10^{11} cm^{-3}, as shown in Fig. 10a. The negative ion densities are reduced by detachment from 10^{11} cm^{-3} to ~10^{10} cm^{-3} or less, as shown in Fig. 10c. The reduction in metastable density is negligible compared with their initial density so that the metastable density is still ~10^{17} cm^{-3}, as shown in Fig. 10d.

Of particular interest is Fig. 10h, showing the electric field to be near zero within the ball. This result follows because the detached electrons make the ball highly conducting, so charges redistribute themselves to make charge currents zero within the ball. Electric fields within the ball then become near zero. The net negative and positive charges to achieve zero field have a complex distribution, as shown in Fig. 10e and f. The ball of electrons has almost zero net motion because of the slight field within the ball. The influence of processes occurring in the sheath boundary tends to change the position of the centre of the ball. The ball of electrons is largely independent of the electrodes as the electrons, positive ions and negative ions and metastable molecules are in close equilibrium with each other.

The formation of the conducting electron ball has a marked effect on potential distributions. During all phases of pulse formation and extinction, the potential 1 cm from the cathode plane is ~4 kV, compared with the driving potential of 14 kV at the centre of the cathode plane; see Figs. 7g and 8g. However, after the formation of the ball, the potential at 1 cm is ~10 kV; see Fig. 10g.

The conducting ball of electrons of Fig. 10a is very different from the more usual conducting balls of plasma that exist between electrodes that are carrying significant current. Because the electric field within the ball is near zero, there is no significant current within the discharge, and an anode and cathode are not necessary. The ball of electrons, together with the background of approximately equal numbers of positive and negative ions that together are electrically neutral, can exist largely independently of the initiating electrodes producing the pulses. These electrons and ions are almost stationary as the electric field is near zero, whereas electrons in a normal discharge typically move with drift velocities of 10^6 cm s^{-1}. Nor do the electrons have thermal energies significantly above that of the cold gas. But the lifetime of the ball is dependent on the supply of metastable molecules, which provide excited molecules to detach electrons from negative ions.

Because the electric field within the ball of electrons produced by metastable detachment is almost zero, heating within the ball will also be very small. Heating depends upon the product of the field and the electron current, and the current itself also depends on the electric field through the dependence of drift velocity on the electric field. Thus, heating depends on the square of the electric field and will be very low.

5. Influence of sheath electric fields at the ball boundary

Section 4 describes how a high density of excited metastable oxygen molecules might be accumulated from successive discharge pulses within a structure. Such metastables have the property of detaching electrons from negative ions and could thus be a source of illumination similar to that in BL. However, each detachment of a negative ion is at the expense of a metastable molecule and metastables are also depleted by quenching through collisions with oxygen molecules. From equation (4), the reciprocal of the time constant for metastable decay, τ, from these two processes, is given by

$$1/\tau = (1/n_m)(dn_m/dt) = -k_q N/5 - k_D \quad n_i \tag{7}$$

Substituting N = 2.5 × 10^{19} cm^{-3} for the total number density of nitrogen and oxygen molecules for air, n_i = 10^{10} cm^{-3}, as found in Figs. 10 and 11, and the values for k_q and k_D, we obtain $\tau \sim 0.1$ s. The ball would consequently only last for less than a second, compared with the usual observations of BL lifetimes of ~10 s. This lifetime still indicates a very significant influence of the metastables as plasma lifetimes of 0.1 s are very much larger than the normal plasma lifetimes of order 1 μs, as obtained in Figs. 7 and 8. However, assuming that the quenching and detachment coefficients k_q and k_D are accurate, we need an additional excitation process for metastable production, to explain observed lifetimes of ~10 s.

Such a process occurs because the ambient electric field causes space charge effects at the surface of the conducting ball that enhance the electric field immediately surrounding the ball. The consequent increases in the electric field have been derived analytically in the classic textbook by Jackson (1962), predicting increases in the background field at the poles of a conducting sphere of a factor of three. These effects are similar to the effect of increases the field at the ends of conducting metal cylinders, which was considered in Section 2. The magnitude of this enhancement can also be estimated by using the derivation of Section 2 by simply substituting E_0R for $E_0L/2$ as the potential that needs to be balanced by the additional field. Thus, the additional field, obtained by substituting R for $L/2$ in the formula for cylinders of $E = E_0L/2R$, is simply $E = E_0$. The ambient electric field is, therefore, expected to be approximately doubled.

We have also estimated these field increases numerically. Fig. 11 shows the electric fields evaluated in the sheath or edge regions at the boundary of the plasma ball. We consider the effect of a uniform ambient electric field of 10 kV cm^{-1} on a ball of metastables of density 5 × 10^{17} cm^{-3} and diameter 4 cm, centred at 5 cm in Fig. 11d. The background densities of negative and positive ions and also metastables are set at 5 × 10^{10} cm^{-3}. Fig. 11a– d shows the densities 10 μs after the introduction of the metastable ball. The electron density is increased from zero to 4 × 10^{10} cm^{-3} and the negative ion density is reduced to 1.8 × 10^9 cm^{-3}, because of the reduction from metastable detachment. The changes to the densities of positive ions and metastable molecules are insignificant in the centre of the ball.

Of central interest in this section are the calculated electric field enhancements in the sheath regions at the edges of the ball shown in Fig. 11h. Along the horizontal axis of the ball, the electric field changes from the ambient field of 10 kV cm^{-1} at the axial position $x = 0$ and increases to 24 kV cm^{-1} at $x = 3$ cm at the edge of the ball, then falls to 0.5 kV cm^{-1} within the ball until the outer edge of the ball at $x = 7$ cm, then increases to 16 kV cm^{-1} in the other sheath region at 8 cm, after

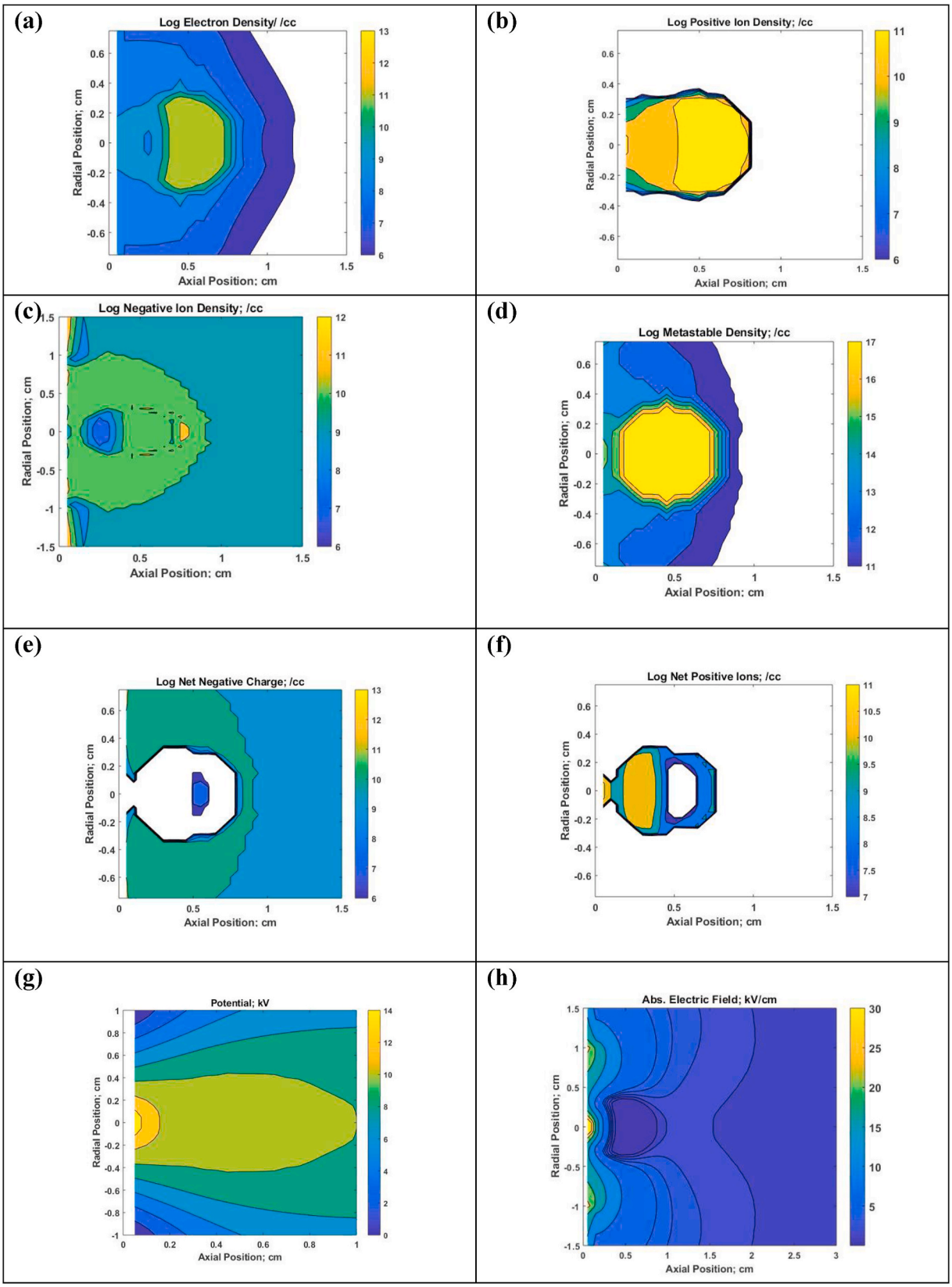

Fig. 10. Calculated distributions of (a) electron density, (b) positive ion density, (c) negative ion density, (d) metastable density, (e) net positive charge density, (f) net negative charge density, (g) electric potential, (h) absolute value of electric field.

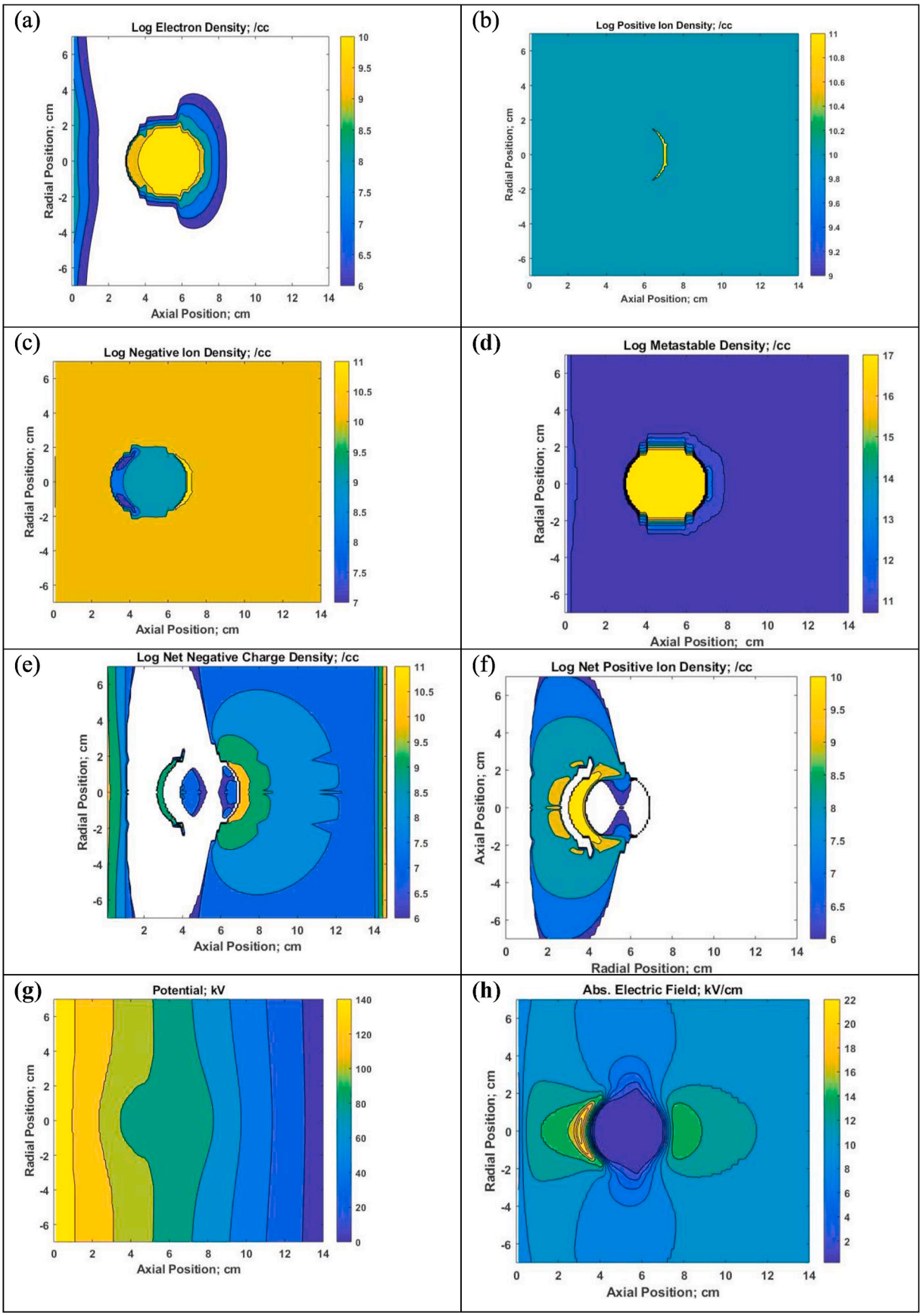

Fig. 11. Calculated distributions of (a) electron density, (b) positive ion density, (c) negative ion density, (d) metastable density, (e) net positive charge density, (f) net negative charge density, (g) electric potential, (h) absolute value of electric field; at ball boundaries.

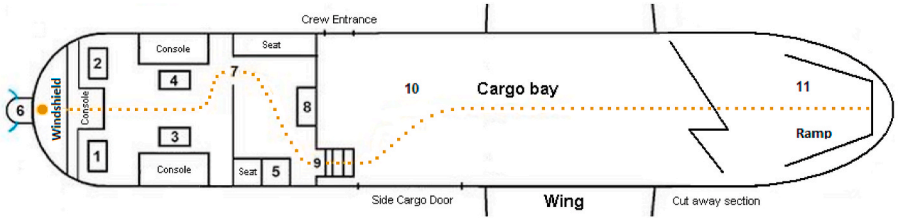

Fig. 12. Ball lightning path within US Air Force plane C-133 A shown by dotted line within cockpit and flight deck. Positions show Pilot 1, Copilot 2, Navigator 3, Flight Engineer 4, Loadmaster 5, Radome 6, with Saint Elmo's Horns, Doorway (open) 7, Coffee console 8, Stairs down to cargo bay 9, Cargo bay 10, Ramp & tail door 11. The ball lightning travelled a total distance of about 55 m from the windshield to the end of the cargo bay in approximately 25–35 s. Drawing by D. Smith, flight navigator.

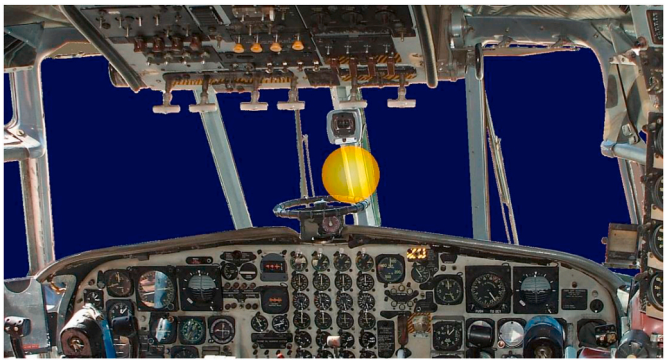

Fig. 13. The ball lightning originated immediately next to the metal divider post at the centre of the windscreen, just under the C-12 standby magnetic compass which was attached near the top of the metal post. The initial position and size of the BL is illustrated by the yellow circle inserted on the photograph.

Fig. 14. Ball lightning in farmhouse. External water tower and plumbing can cause large electric fields inside house from fields during thunderstorms.

which the field decreases back to the average value of 10 kV cm^{-1} far away from the ball. Fields as low as 2 kV cm^{-1} are sufficient to excite metastables, as shown in Fig. 1, and fields of 25 kV cm^{-1} can produce ionization. These calculations show that large ambient electric fields can be accentuated in the sheath by about a factor of two, in agreement with the approximate analytic derivation. The fields are certainly sufficient for the further excitation of metastables and, for high ambient fields, would be sufficient for further ionization. Thus the lifetime of the ball would be increased beyond the calculated quenching limit of 0.1 s, and there would also be an explanation of the motion of the ball.

The magnitude of the ambient electric field, 10 kV cm^{-1}, is large and would amount to a potential of 50 kV over a distance of 5 cm. Such potentials are, however, smaller than the typical potentials produced by lightning of 1 MV, and potentials a tenth of 1 MV would be sufficient to enhance metastable excitation in the sheath.

Fig. 10e and f and also Fig. 11e and f shows the net positive and negative charges within the ball calculated to produce a zero or low field in the conducting ball. They have complex distributions and will vary as a function of time. The calculations of Fig. 11 have been repeated for a thundercloud ball radius of 20 m, an increase of a factor of 1000 from the ball radius of 2 cm of Fig. 11. The calculated field intensity increase was again approximately a factor of two, supporting the analytic formula and indicating that the increase is independent of ball radius.

6. Discussion

Despite the shortcomings in our model, which we discuss below, our calculations suggest that it may be possible to explain the principal properties of BL observations in houses and aircraft from gas discharge behaviour, provided that the effects of metastable oxygen molecules are considered.

(1) The BL properties only occur for large metastable densities, of the order of a few percent of the total gas density, and it takes the order of seconds for such densities to accumulate in the discharge. For numerical stability, the time steps of the calculations cannot be more than the transit time for electrons to cross a mesh cell. In our calculations, time steps were typically 10^{-9} s, so it is not practical to continue time-dependent calculations beyond the initial stages of the discharge. We have predicted the influence of the large metastable densities by arbitrarily introducing a cloud with a high metastable density without calculating a detailed time dependence.

(2) Very approximate order of magnitude calculations have been made to compare the input electrical energy for the model with the energy of BL as assessed from observations in houses and aircraft. The input energy is in two components. The first is the energy of the ball of metastables, which follows from the energy density of the metastable particles in the ball, i.e. $n_m Ve$. The energy of excitation, V, of the metastable singlet delta oxygen molecules is ~1 eV, and the metastable particle density n_m has a maximum value of 0.5×10^{19} cm^{-3}, obtained assuming that all oxygen molecules are in the metastable state, the total particle density for air at 1 bar being 2.5×10^{19} cm^{-3}. The approximate particle energy density is thus ~0.5 J cm^{-3}. The second component of the input energy is from energy gained from the sheath electric fields during the continuous discharge phase, as described in Section 5, which is very difficult to determine.

Two types of observation allow the BL energy to be estimated. Firstly, there are many observations that the light output of BL within houses is about that of a 100 W incandescent light bulb. Thus, for the approximate energy density required to produce the emitted radiation we multiply 100 W by the ball lifetime of 10 s, by a factor of 0.03 to account for the low radiative efficiency of incandescent lamps and divide by 500 cm^{-3}, the approximate volume of a ball of diameter 10 cm. The resultant energy density ~0.1 J cm^{-3}, compared with the possible energy density of the ball of 0.5 J cm^{-3}, indicating that the metastable particles are capable of supplying the required radiation energy. The energy magnitudes are approximately consistent.

A second indication of the possible magnitude of BL energy is that

there are many observations of BL ending with an explosive bang. Descriptions of the magnitude of the "bang" vary from a "pang" or no bang at all, see Appendix 2, to "like a rifle shot" (see Lowke, 1996). Almost always, there is no damaging explosion. Our BL model leads to a possible explanation of such an explosive termination because metastable oxygen molecules dissociate at high temperatures, liberating their energy to the gas. Thus, any heating of BL could lead to metastable dissociation, producing still further heating, and thus an explosive runaway is possible. An energy of 0.5 J cm^{-3} would lead to heating air by ~120 K, significantly increasing the local gas pressure and producing a bang.

(3) We have not presented a detailed account of radiation emission. Nevertheless, from the evidence presented in Ionin et al. (2007), mentioned in the introduction, radiation of wavelength 762 nm in the red region of the spectrum will be emitted from the ball from binary collisions of metastable molecules and at ~ 500 nm in the yellow region of the spectrum from collisions of three metastable molecules. Furthermore, in the sheath regions at the edge of the ball, electric fields approach ionization fields, and visible radiation will be emitted.

(4) From the analysis of ball behaviour in Section 5, the ball motion strongly depends on the ambient electric field as determined by both background fields and by any modifications to the electric field caused by ions ejected from the ball. If ambient fields were zero, from Section 5, the ball would be extinguished in less than a second because there would be no replenishment of metastable molecules from the sheath fields. The absence of strong ambient fields in typical experiments designed to produce BL might explain the inability to produce BL. Our results suggest that for BL to exist for more than a second a background ambient field is necessary.

(5) The extensive and complex movement of the ball illustrated in Fig. 12 strongly suggests there is an influence of electrostatic fields formed from ions emitted from the ball and collected on insulating walls. Potentials inside of an aircraft with a conducting fuselage are likely to be uniform, as in a Faraday cage, and at about the potential in the atmosphere at the centre of the aircraft. But potentials outside the aircraft vary considerably after any lightning strike. Average lightning strikes deliver a charge $Q =$ 30 C. Even after this charge is spread over a sphere of radius R of 1 km, the resulting perturbation in the local potential from this charge is ~300 MV, as follows from the electrostatic relation $V = Q/(4\pi\varepsilon_0 R)$. Fields due to the difference between the potentials, for example between the inside and outside of the front of the fuselage, will be a significant driving force to disperse charges from the BL discharge. This will change potentials within the aircraft through the collection of charges on the insulating walls, producing electric fields inside the aircraft.

(6) We suggest that the observation reported by Selvaggi et al. (2003) of BL that came from a fireplace and caused significant human injury, may have been formed inside the fireplace rather than coming down the chimney from outside the house. If the chimney had an internal metal flue pipe, or even if it was without a flue pipe and there was a carbon coating inside, the chimney would have been an approximate vertical conducting cylinder as described in Section 2. Then amplification of any thundercloud field in the fireplace would have occurred by a factor of approximately the ratio of the chimney height to its radius. This enhanced field would have been over a much larger volume than the fields of a few mm discussed in Figs. 7 and 8, and any BL produced would have a very much larger total energy than usual. The BL initiation would still be consistent with the proposed mechanism involving metastables.

(7) The metastable initiation mechanism of BL gives an explanation for the reliable observation in Neuruppin, Germany, where over a dozen BLs were formed almost simultaneously with a lightning strike. These BLs were at distances of 5 km or more from the point of the lightning strike (Baecker et al., 2007). This lightning strike was exceptionally large. It was measured by the Siemens lightning detection network to have a current of the order of 370,000 A; the average lightning strike has a current of 30,000 A. Such a large current would significantly distort the local potential of the ground near the lightning strike. This perturbation would be transmitted to the local town 5 km away from the strike by large potential differences between local metallic plumbing and electrical power lines, and the local ground potential at many points in the town. Large differences in potential between points on water taps, for example, and the local ground potential, would cause electrical discharges to be initiated at points on the tap, as described in Section 2. Metastables would then be produced as described in Section 3.

(8) The present paper is concerned with the properties of BL within houses and aircraft. However, the results are also relevant to wider aspects of the physics of lightning and gas discharges generally. An example is the cloud structure and physical processes contributing to high-energy photons and gamma rays, as discussed by Chilingarian et al. (2019). It is also relevant to the understanding of the large plasmoids produced above water, and frequently initiated below water, as discussed, for example, by Friedl et al. (2020). Plasma initiation is also relevant to the work of Ohtsuki and Ofuruton (1991) who generated fireballs by interference of microwaves.

7. Summary and conclusion

This paper investigates the possibility of ball lightning being produced by an electrical discharge in structures such as a house or aircraft. Four separate stages of gas discharge development are proposed.

(1) A conductor, such as a pipe or metal column within a house, or an aircraft fuselage itself, increases the ambient electric field from a thundercloud near the tips of the conductor and may produce ionization. The field enhancement factor is approximately given by the ratio of the length to the diameter of a cylindrical conductor.

(2) Pulsed corona discharges in this high-field region produce excited metastable states of oxygen, namely the singlet delta state, which has the property of detaching electrons from negative ions.

(3) Accumulated metastable densities of the order of 10^{17} cm^{-3} detach electrons from negative ions, producing electron densities of ~10^{11} cm^{-3} in a cloud or ball. The electric field within the ball is almost zero, and the ball's motion is largely independent of the electrodes.

(4) Sheath fields develop at the edges of the ball to match the ball potential with the ambient potential. The sheath fields excite additional metastable molecules that increase the lifetime of the ball.

It is concluded that it may be possible to explain properties of ball lightning that occurs inside of houses and aircraft in terms of conventional gas discharge theory.

Declaration of competing interest

The authors declare that they have no known competing financial interests or personal relationships that could have appeared to influence the work reported in this paper.

Acknowledgements

The authors would particularly like to acknowledge the contributions of Mr Don Smith, retired from the US Airforce, who was the

navigator of the C-133 A cargo aircraft when ball lightning occurred. Smith's report of the detailed conditions of the formation and subsequent transit of the ball are given in Appendix 1. He also contributed Figs. 4, 12 and 13. JJL is grateful to Dr M L Shmatov of the Ioffe Inst. St Petersburg for informing him of the early work of Powell and Finkelstein and also the recent work reported in the paper of Shmatov and Stephan. JJL is also grateful for significant computer science contributions from his son Russell.

Appendix A. Observation of ball lightning in US Aircraft C-133A in 1960s

Don Smith, Navigator, retired, US Air Force

In the mid-1960s, I was a Lieutenant in the US Air Force and was the crew Navigator aboard a C-133 A cargo aircraft flying from California to Hawaii. We were at an altitude of 18,000 feet, it was at night, and we were flying in a continuous horizontal layer of thin cloud which had the density of "soup". The C-133 A had four propellers driven by four turbine engines and, at the time was the U.S. Air Force's largest cargo aircraft. On the nose of the C-133 A there was a radome that was visible from inside the cockpit. The radome was a dome-shaped shell used to cover the radar antenna and was about 36 inches across and had a rounded dome front. As Navigator, I was monitoring the radar for any significant weather clouds in front of us. There was only the fog.

After we had been flying in the fog for about 15 min, there developed on the radome two horns of Saint Elmo's fire. It looked as if the airplane now had bull's horns on the radome. The curved horns, each about a foot long, were glowing with the blue of electricity. The two Pilots, the on-duty Engineer and I enjoyed watching and discussing the horns for a relatively long time. The horns were not at all of concern as we had seen Saint Elmo's fire several times previously when in similar flight weather conditions. We thought of it simply as static electricity. These horns are illustrated in blue in Fig. 4.

The on-duty Engineer and I were standing behind the pilots as we all were actively discussing the Saint Elmo's fire decorating our radome. Suddenly, within sight of all four of us – we were all looking at the horns – a glowing ball of golden fire about the size of a volleyball appeared just inside the windshield, midway of the windshield and above the central Pilot console. It touched nothing and made no sound (or none that could be heard above the usual airplane noise) but slowly floated downward into the cockpit between the Pilots, then between the Engineer and me, coming within a foot of me at my waist, now staying about three feet above the floor, then slowly turned left toward the crew lounge doorway, went through the open doorway, turned right 90° and toward where the Loadmaster was sitting. We, the Pilots, the Engineer and I lost sight of it then because of the wall between the cockpit and the crew lounge. About 20 s later, the Loadmaster burst into the cockpit yelling "Did you see THAT ???" The Loadmaster said that he saw a ball of golden fire come from the cockpit into the crew lounge. It floated toward him, came within a foot of him but turned to exit through the open stairway door and down the stairway into the cargo bay - then to float above the cargo down the exact middle of the airplane toward the tail of the airplane - and then just disappeared as it went through the metal tail ramp & door at the rear of the airplane. We all exchanged what we each had seen, confirming with each other that we had seen the same thing. We told the second Engineer, who had slept through the event, all the details. The Engineers and Loadmaster searched for any damage to the airplane and, finding no damage, we continued the flight uneventfully.

The path of the Ball inside of the plane is illustrated in Fig. 12. The position of the formation of the Ball at the Pilot's windshield is illustrated by the yellow circular region inserted on the photograph of Fig. 13. The ball lightning appeared in an instant inside the cockpit and was centred at the vertical metal post located in the exact centre of the windscreen. The ball appeared on our side of the metal post and the ball's centre was on the post and was not over any part of the glass of either windscreen window. The ball was not bright like looking at a naked light bulb. It was like looking at a gentle or medium fire in a fireplace. It did not illuminate the cockpit but was like looking at a pumpkin ball of orange color that did not illuminate its surrounding but was clearly visible. The ball seemed to "float" along and was not moving fast, but in a steady determined pace.

Upon landing at Hickam AFB in Hawaii, the Pilot directed Maintenance to search the aircraft inside and outside for any sign of lightning damage. No damage was found. The crew made a detailed written report of the incident to the Base Command Post.

At no time during this flight were there any thunderstorms along our route. We were flying through a fog-like layer of cloud, and there was no turbulence. We never saw any lightning outside the aircraft, neither close by nor in the distance. We did not see any lightning flash whatsoever. No individual clouds ever appeared on the radar which I was monitoring closely; only a pea-soup-like fog layer was evident. The radar was at full power during the time that the St. Elmo's horns and the ball lightning occurred and the radar beam was in the narrow Pencil shape. The ball lightning appeared about halfway between Travis AFB in California and Hickam AFB in Hawaii.

The flying altitude was 18,000 ft, and the cabin altitude will have been set to the atmospheric pressure at 8000 ft or somewhat above. From the approximate location and the NOAA weather database, we can estimate that the outside temperature will have been around −15 °C. It is very probable that the layer of fog consisted of ice crystals. Of particular interest is that the ball lightning was preceded for some minutes by the observation of corona outside of the airplane. No observation was made of the ball lightning having any existence outside of the airplane.

Appendix B. Observation of ball lightning in a farmhouse

Peter Coe, USA.

Source: https://www.quora.com/Have-you-ever-witnessed-ball-lightning.

In 1969 or so my parents purchased an old ramshackle farmhouse on a hilltop in Northwestern Massachusetts as a vacation home. Our first summer up there the house had not been renovated yet. It had no lightning rods despite being in a field on top of a hill. There was a rusty iron deep-basin sink in the corner of the dining room, and sometimes during the violent thunderstorms that were frequent that summer, ball lightning or "fireballs" as we called them would come out of the faucet. They would come out one after another with a loud "Pang!Pang!Pang!" and then skitter around in the sink for a few seconds before disappearing in another loud "Pang!" I remember them as being about 3–4 inches in diameter and orangey in color making a lot of sparks as they skittered around the sink. My father would always yell "Get away from the sink! Don't touch anything metal!" A friend of our family who was a physics professor at Yale came over to dinner one night and was absolutely thrilled to see this phenomenon! Apparently he been trying to create plasma balls in his lab for some time, and here it was happening in an old rusty farm sink! At age five I though[t] this was just something that normally occurred. After the house was renovated, the iron sink was removed and lightning rods were installed, this phenomenon has never happened again. Thinking about it now, I think that the frequency of the fireballs happened with the dripping of the old tap. Perhaps the individual drops of water had become supercharged with electricity by the lightning strikes all around the house?

Fig. 14 shows a photograph of a house with an external water tank and metal plumbing which can cause accentuated electric fields inside of a house because of the mechanism outlined in Section 2.

References

Abrahamson, J., Dinnis, J., 2000. Ball Lightning caused by oxidation of nanoparticle networks from normal lightning strikes. Nature 40, 519–521.

Baecker, D., Boerner, H., Naether, K., Naether, S., 2007. Multiple ball lightning observations at Neuruppin, Germany. Int. J. meteorology 32 (No. 320), 193–198.
Bauer, G., Graves, D.B., 2016. Mechanisms of selective antitumor action of cold atmospheric plasma-derived oxygen and nitrogen species. Plasma Process. Polym. 13, 1157–1178.
Bychkov, V.L., 2002. Polymer-composite ball lightning. Phil. Trans. Roy. Soc. Lond. 360, 37-6.
Chilingarian, A., Hovsepyan, G., Elbekian, A., Karapetyan, T., Kozliner, L., Martoian, H., Sargsyan, B., 2019. Origin of enhanced gamma radiation in thunderclouds. Phys. Rev. Res. 1, 033167.
Corum, K.L., Corum, J.F., 1990. High voltage rf ball lightning experiments and electro chemical fractal clusters. In: Also Presented at 2nd International Conference on Ball Lightning, Budapest, Hungary, 26–29 June 1990, pp. 47–58. Usp Fiz. Nauk 47, 160 (4).
Dubinova, A., Rutjes, C., Ebert, U., Buitink, S., Scholten, O., Trinh, G.T.N., 2015. Prediction of lightning inception by large ice particles and extensive air showers. Phys. Rev. Lett. 115, 015002.
Findlay, F.D., Snelling, D.R., 1971. Collisional deactivation of $O_2(^1\Delta_g)$. J. Chem. Phys. 55, 545–550.
Friedl, R., Fantz, U., Pilottek, I., Schmid, D., Steibel, S., 2020. Spatio-temporal structure and emission of a large plasmoid in atmosphere. J. Phys. D (in press). https://iopscience.iop.org/article/10.1088/1361- 6463/abc918.
Ionin, A.A., Kochetov, I.V., Napartovich, A.P., Yuryshev, N.N., 2007. Physics and engineering of singlet delta oxygen production in low-temperature plasma. J. Phys. D Appl. Phys. 40, R25–R61.
Jackson, J.D., 1962. Classical Electrodynamics, Classical Eletrodynamics, Chapter 2. John Wiley and Sons, Inc., New York, London equation 2.15.
Karch, C., Calomfirescu, M., Rothenhausler, M., Brand, C., Meister, H., 2017. Lightning Strike Protection of Radomes – an Overview. Deutscher Luft und Raumfahrtkongress. Document ID 450139.
Kearns, D.R., 1971. Physical and chemical properties of singlet molecular oxygen. Chem. Rev. 1971 71 (4), 395–427.
Lowke, J.J., 1992. Theory of. Electrical breakdown in air- the role of metastable oxygen molecules. J. Phys. D: 25, 202–210.
Lowke, J.J., 1996. A gas discharge theory of ball lightning. J. Phys. D Appl. Phys. 29, 1237–1244.
Lowke, J.J., Smith, D., Nelson, K.E., Crompton, R.W., Murphy, A.B., 2012. Birth of ball lightning. J. Geophys. Res. 117, D19107.
Lowke, J.J., 2019. From switching arcs to Ball Lightning to curing cancer. Plasma Technology 6 (2), 194–199.
Morrow, R., 2018. General theory for ball lightning structure and light output. J. Phys. D Appl. Phys. 51, 125205.
Morrow, R., 2019. The origin of ball and bead lightning from an expanded lightning channel. J. Atmos. Sol. Terr. Phys. 195, 105116.
O'Doherty, J.J., 1944. Diffusion phenomena in alternating current arcs. Nature 153 (No. 3888), 558-558, also 154, No. 3906, 339.
Ohtsuki, Y.H., Ofuruton, H., 1991. Plasma fireballs formed by microwave interference in air. Nature 50, 139–141.
Piccoli, R., Blundell, R.A., 2014. Statistical Study of Ball Lightning Events Observed in France between 1994 and 2011, vol. 6. Unconventional Electromagnetics and Plasmas, New Delhi, India, pp. 1–2.
Powell, J.R., Finkelstein, D., 1969. The structure of ball lightning. Adv. Geophys. 13, 141–189.
Selvaggi, G., Monstrey, S., von Heimburg, M., Hamdi, M., Van Landuyt, K., Blondeel, P., 2003. Ann. Plast. Surg. 50 (No. 5), 541–544.
Shmatov, M.L., Stephan, K.D., 2019. Advances in ball lightning research. J. Atmos. Sol. Terr. Phys. 195, 105115.
Shmatov, M.L., 2020. Possible detection of visible light and γ rays from a swarm of ball lightning. Phys. Rev. E 102, 013208.
Sousa, J.S., Bauville, G., Puech, V., 2013. Arrays of micro-plasmas for the controlled production of tunable high fluxes of reactive oxygen species at atmospheric pressure. Plasma Sources Sci. Technol. 22, 035012.
Tesla, N., 1944. Colorado Springs Notes 1899–1900 (Published in USA after Tesla's Death, pp. 368–370.
Trichel, G.W., 1938. The mechanism of the negative point to plane corona near onset. Phys. Rev. 54, 1078–1084.